

# Simulated and observed fluxes of sensible and latent heat and CO<sub>2</sub> at the WLEF-TV tower using SiB2.5

IAN BAKER\*, A. SCOTT DENNING\*, NIALL HANAN†, LARA PRIHODKO\*, MAREK ULIASZ\*, PIER-LUIGI VIDALE‡, KENNETH DAVIS§ and PETER BAKWIN¶

\*Department of Atmospheric Science, Colorado State University, Fort Collins, CO 80523-1371, USA, †Natural Resource Ecology Laboratory, Colorado State University, USA, ‡Institute for Atmospheric and Climate Science, ETH, Zurich, Switzerland §Department of Meteorology, The Pennsylvania State University, USA, ¶Climate Monitoring Diagnostics Laboratory, National Oceanic and Atmospheric Administration, Boulder, CO, USA

## Abstract

Three years of meteorological data collected at the WLEF-TV tower were used to drive a revised version of the Simple Biosphere (SiB 2.5) Model. Physiological properties and vegetation phenology were specified from satellite imagery. Simulated fluxes of heat, moisture, and carbon were compared to eddy covariance measurements taken onsite as a means of evaluating model performance on diurnal, synoptic, seasonal, and interannual time scales. The model was very successful in simulating variations of latent heat flux when compared to observations, slightly less so in the simulation of sensible heat flux. The model overestimated peak values of sensible heat flux on both monthly and diurnal scales. There was evidence that the differences between observed and simulated fluxes might be linked to wetlands near the WLEF tower, which were not present in the SiB simulation. The model overestimated the magnitude of the net ecosystem exchange of CO<sub>2</sub> in both summer and winter. Mid-day maximum assimilation was well represented by the model, but late afternoon simulations showed excessive carbon uptake due to misrepresentation of within-canopy shading in the model. Interannual variability was not well simulated because only a single year of satellite imagery was used to parameterize the model.

*Keywords:* Land-atmosphere interactions, carbon flux

*Received 15 February 2002; revised version received 15 April 2003 and accepted 22 April 2003*

## Introduction

The land-surface is an important source and sink of radiation, sensible heat, water, momentum, and trace gases to the atmosphere. A parameterized representation of these exchanges is an important component in all climate and weather models (Betts *et al.*, 1996). Land-surface parameterizations have undergone tremendous development in the past decade, and now include a much greater degree of biophysical realism and self-consistency than was being used just a few years ago (Sellers *et al.*, 1997). Biophysically based land-surface parameterization has been shown to lead to better ability of numerical weather prediction (NWP) models to forecast weather under extreme climatic conditions such as droughts (Atlas *et al.*, 1993) and floods (Beljaars *et al.*, 1996). Land-surface parameterization is an

important part of the numerical weather analysis and forecasting infrastructure at the European Center for Medium-Range Weather Forecasting (Viterbo *et al.*, 1995). Land-surface predictions can also be used to evaluate the accuracy of and develop better parameterizations for assimilation of weather and climate data (Betts *et al.*, 1998).

A new generation of land-surface parameterizations has emerged in recent years in which exchanges of water and heat at the vegetated land surface are linked to exchanges of CO<sub>2</sub> (Sellers *et al.*, 1997). This linkage is based on the fact that physiological control of evapotranspiration by plants is an evolved optimization mechanism that maximizes photosynthetic carbon fixation (by drawing CO<sub>2</sub> into leaves through stomatal pores) for a minimal amount of water loss from the plant (by stomatal adjustment). The representation of this linkage in land-surface parameterizations has been shown to improve the simulated diurnal cycle of

Correspondence: Kenneth Davis, e-mail: davis@essc.psu.edu

temperature and humidity. It also allows key parameters controlling surface exchanges to be related to the spectral reflectance characteristics of vegetation (Sellers *et al.*, 1992; Sellers *et al.*, 1996a,b). This carbon-water linkage also opens the door for the models to predict the flux of CO<sub>2</sub> in a self-consistent way with simulated surface energy exchanges and turbulent and convective transport in the atmosphere. By coupling photosynthesis and energy flux calculations with an atmospheric transport model, Denning *et al.* (1996a,b) were able to achieve a greater degree of realism in simulated diurnal and seasonal variations of CO<sub>2</sub> than had previously been possible.

Atmospheric trace gas concentration fields contain information about the surface exchanges of these gases. This information can be interpreted using numerical transport models to deduce large-scale sources and sinks of CO<sub>2</sub>, for example. A recent 'inversion' study of this kind (Fan *et al.*, 1998) suggests that biological processes at the land surface currently remove an enormous amount of CO<sub>2</sub> from the atmosphere over North America. Similar analyses by other modeling groups have found the North American sink to be much smaller (Bousquet *et al.*, 1999a,b; Rayner *et al.*, 1999; Gurney *et al.*, 2002). Such analyses depend sensitively on the representation of the linkages among photosynthesis, heat fluxes, convective motions, and large-scale transport in the atmospheric models (Denning *et al.*, 1995, 1996b, 1999). Realistic land-surface parameterizations are therefore crucial for interpreting large-scale CO<sub>2</sub> concentration fields in terms of the locations and processes responsible for the fluxes of greenhouse gases.

In this paper, we evaluate the performance of a land-surface parameterization (SiB2.5) that has been used in an atmospheric GCM and in a mesoscale atmospheric model. Unlike some previous studies comparing SiB performance to observations (Sellers & Dorman, 1987; Sellers *et al.*, 1989; Colello *et al.*, 1998; Sen *et al.*, 2000), we made no effort to 'tune' model parameters to improve the agreement with the observations. The state of the canopy in the model therefore represents our best ability to represent the actual canopy as derived from remote satellite observations and soil/vegetation maps, and is analogous to the use of the model to simulate regional fluxes when coupled to a mesoscale model (see Denning *et al.*, this issue) or a global model (see Denning *et al.*, 1996b).

## Methods

### Model description

The Simple Biosphere (SiB) Model, originally developed by Sellers *et al.* (1986), was substantially modified

(Sellers *et al.*, 1996a), and has since been referred to as SiB2. The number of biome-specific parameters was reduced, and most are now derived directly from processed satellite data (Sellers *et al.*, 1996b,c), rather than prescribed from the literature. Another major change is in the parameterization of stomatal and canopy conductance used in the calculation of the surface energy budget over land. This parameterization involves the direct calculation of the rate of carbon assimilation by photosynthesis (Farquhar *et al.*, 1980), making possible the calculation of CO<sub>2</sub> exchange between the global atmosphere and the terrestrial biota on a time step of several minutes (Denning *et al.*, 1996a,b; Zhang *et al.*, 1996). Photosynthetic carbon assimilation is linked to stomatal conductance and thence to the surface energy budget and atmospheric climate by the Ball-Berry equation (Collatz *et al.*, 1991, 1992), which is the basis for the ability of the model to calculate the climatic effects of physiological responses to elevated CO<sub>2</sub> (Sellers *et al.*, 1996c). Soil respiration is calculated from the temperature and moisture of each layer of soil, and is scaled to achieve carbon balance over an annual cycle (Denning *et al.*, 1996a). Recent improvements include the introduction of a six-layer soil temperature submodel based on the work of Bonan (1996, 1998), and a revised surface energy budget that includes prognostic temperature, moisture, and CO<sub>2</sub> in the canopy air space reservoir. We refer to the revised model as SiB2.5.

Modeled fluxes of heat, water vapor, and carbon are dependent not only on meteorological drivers (temperature, humidity, wind, and precipitation) but are also highly dependent on the characteristics of the canopy vegetation and soil type. In mid-latitudes especially, leaf area index (LAI) is highly correlated with carbon flux, and soil texture has a strong impact on heat and water fluxes. A major difference between SiB2.5 and many other land surface schemes is in the specification of vegetation and soil parameters. These parameters are commonly specified as monthly values tied to vegetation type through a 'look-up table' (e.g., Bonan, 1998), whereas SiB specifies LAI, absorbed fraction of photosynthetically active radiation (FPAR), and greenness fraction from normalized difference vegetation index (NDVI) derived from satellite imagery. The result is that although SiB defines a small number of biome types within its parameter set, use of the observed NDVI values creates spatial heterogeneity in canopy properties even over large areas of vegetation classified as a single type.

Vegetation and soil physical parameters were specified using a combination of land cover type (Hansen *et al.*, 2000), monthly maximum NDVI derived from advanced very high resolution radiometer (AVHRR)

data (Teillet *et al.*, 2000), and soil properties (STATSGO, 1994). Time-invariant vegetation biophysical parameters such as canopy height, leaf angle distribution, leaf transmittance, and parameters related to photosynthesis, are based on values recorded in the literature and assigned via look-up tables. Time-varying vegetation biophysical parameters such as FPAR, fraction of vegetation cover, greenness fraction, and LAI are calculated from 1 year of NDVI monthly maximum value composites for the site. The time-varying parameters are based on equations in Sellers *et al.* (1992, 1996b) and Los *et al.* (2000). Soil hydraulic and thermal parameters are calculated from the percent of sand and clay in the soil using equations from Clapp and Hornberger (1978).

A representative footprint was extracted from each of the 12 months and the time-varying calculations as well as the respiration calculation were performed on the average NDVI for that footprint. This footprint was meant to incorporate the primary source region of the measured fluxes, and was consistent with numerical simulations of footprints for this height performed with the aid of a Lagrangian particle model. The simulations were performed for several cases of the convective boundary layer where the particle model was driven by the large eddy simulation output from CSU RAMS (Regional Atmospheric Modeling System) (Uliasz, 2000). An average wind speed and direction was determined, and estimated footprints from the mesoscale modeling studies were used to determine which pixels from the NDVI image should be used. Both the areal coverage and orientation around the tower site were taken into consideration. The chosen NDVI image pixels were then averaged together to obtain a mean NDVI value, which was passed into the code that produced the boundary condition data. It was found that the composite NDVI values were fairly insensitive to the footprint size within the immediate WLEF area; composite NDVI values were almost identical between footprints of 24 and 9 km<sup>2</sup>.

#### *Observational dataset*

The WLEF-TV tower is located in north-central Wisconsin, USA, near the town of Park Falls. The tower is a 447-m tall television transmitter (WLEF TV 45°55'N, 90°10'W) located in the Chequamegon National Forest, 14-km east of Park Falls. The region is in a heavily forested zone of low relief. The region immediately surrounding the tower is dominated by boreal lowland and wetland forests typical of the region. Much of the area was logged, mainly for pine, during 1860–1920, and has since regrown. The concentration of CO<sub>2</sub> has been measured continuously at six heights (11, 30, 76, 122,

244, and 396 m above the ground) since October 1994, and CO<sub>2</sub> flux has been measured since May 1995, and at three heights (30, 122, and 396 m) since early 1996 (Berger *et al.*, 2001). Micrometeorology and soil temperature and moisture data were collected at the site or at the nearby USDA Forest Sciences Laboratory. These measurements have been reported by Bakwin *et al.* (1998) and in many of the companion papers in this special issue.

The meteorological measurements required to drive SiB2.5 include near-surface temperature, humidity, incoming solar and long-wave radiation, wind speed, and precipitation. For this study, these data were defined directly using measurements averaged at 30-min intervals at the tall tower site. Incoming long-wave radiation was not measured, so the method of Idso *et al.* (1981) was used to estimate long-wave radiation from air temperature and humidity. The driver data were incomplete because of intermittent instrument or data-logger failures. Since the model requires unbroken series of driver data, data gaps were filled using a hierarchical set of methods that included interpolation within the data set and use of alternative measurements made at the WLEF site and at a nearby meteorological station (Willow Springs).

The gap-filling sequence included, in order of preference: (1) temporal interpolation within the data stream for gaps of less than 2 h, (2) use of data from an alternative height on the WLEF tower, with adjustment for systematic differences caused by height, (3) use of data from Willow Springs, with adjustment for systematic differences caused by location, (4) use of an average for the time of day of missing measurements, using data from the previous and following 15-day period, and (5) use of an average for the time and date of missing measurements, using data from the previous and following 15-day period, in the same year and any other available year. In methods (2)–(5) the mean adjustment and averages were calculated, with standard deviations, using measurements at that time of day during the 15-day period before and after the time and date of the missing measurement. To increase confidence in the filled data, methods (2)–(5) were not used if the variability of the adjustment or average was more than a threshold value (defined as standard deviation/mean = 2.0). In the case of solar radiation and precipitation, where multiple measurements were not available on the tall tower, method (2) was not available. In the particular case of precipitation, the spatial and temporal variability of the process is such that no adjustment for location was attempted and measurements at Willow Springs were used directly during data gaps at WLEF. During the wintertime, the WLEF and Willow Springs gauges had problems

recording snowfall events. To produce more accurate snowfall driver data, snowfall observations from Rhinelander WI (40 miles southeast of the WLEF tower) were used to determine wintertime precipitation driver data. The daily observation of Rhinelander precipitation provided no information as to the intensity breakdown during the previous 24 h, and so was divided into equal hourly increments with the assumption that winter precipitation would be generally stratiform in nature.

For the present study, SiB was run in the offline mode to compare model fluxes with WLEF observations taken between 1997 and 1999. 122 m was used as the 'above-canopy' height, and data recorded at that level as the driver data for SiB. The WLEF dataset provided a large number of observations of sensible ( $H$ ) and latent heat ( $LE$ ), as well as net ecosystem exchange ( $NEE$ ) of carbon between the canopy and the boundary layer.  $NEE$  and latent and sensible heat fluxes were calculated for three levels (30, 122, and 396 m) on the tower, with a correction term added for heating/moistening of each layer. Because of the multiple-level and high-altitude flux and mixing ratio data, as well as clearing around the base of the tower, an algorithm was developed that selected one or more of the multiple measurements for each hourly flux value. Data were taken from 122 and 396 m under strongly unstable conditions (surface sensible heat flux greater than  $100 \text{ W m}^{-2}$ ), and from 30 m under stable to slightly unstable conditions. If the preferred levels were missing, data were taken from any existing turbulent flux level. One and two hour data holes were interpolated. Observations were taken hourly, while SiB output was averaged from the 10-min model time step to hourly output, to correspond with the observational time step.

## Results and discussion

The model results presented here are 'untuned', in that no directly observed canopy information is used. All vegetation and soil parameters were obtained from satellite information and previously published maps. Model output was analyzed as is: we did not iterate through runs and modify model parameters until the best match to the observations was found. We looked at model output across temporal scales from time series of individual days to monthly diurnal composites and monthly means.

### *Synoptic and diurnal scales*

During the summer months, both respiration and assimilation fluxes reached their largest values of the year. Warm, moist soil provided optimum conditions

for respiration, and by June (all years) the canopy was in full leaf and the highest LAI values of the year were seen. SiB performance during the summer months (June, July, and August) was quite reasonable with regard to  $LE$  and  $NEE$ , but model  $H$  exceeded the observed values by a considerable margin. Figure 1 shows diurnal composites of monthly  $LE$  for the 3 years simulated. Simulated fluxes capture the observed variation with no obvious bias. The exception to this is 1998, when the modeled transpiration rates were close to 1997 and 1999 levels while the actual forest was drying out. In that year the forest around WLEF came into full leaf early in the season, and dried out during the summer – by late June, the forest floor was described as 'crunchy when walked upon' by observers. In the model simulations, there was no calculated water stress on the vegetation and during this time-transpiration was comparable to 1997 and 1999 levels (July mid-day  $NEE$  near  $-12$ ; Fig. 7). Meanwhile, eyewitness observers (as mentioned above) and flux data (Figs 1–3 and 7) indicate that the forest was stressed; Bowen ratio was higher than July 1997 or 1999, and mid-day  $NEE$  was larger as well.

The simulated sensible heat flux (Fig. 2) did not compare well with observations in the summer months.

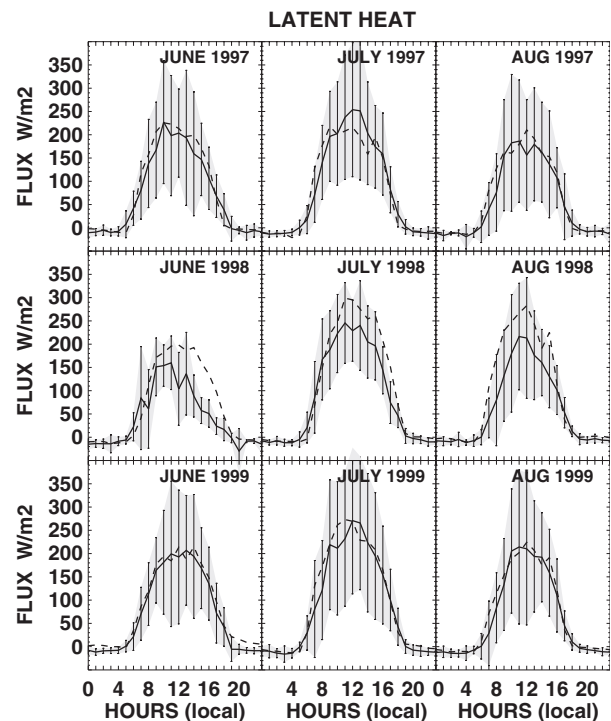


Fig. 1 Diurnal composites of model and observed latent heat fluxes for summer months during the years 1997–1999. In all panels model data is the dashed line, observed the solid line. Shaded area indicates  $\pm 1$  standard deviation of the mean of the observations.

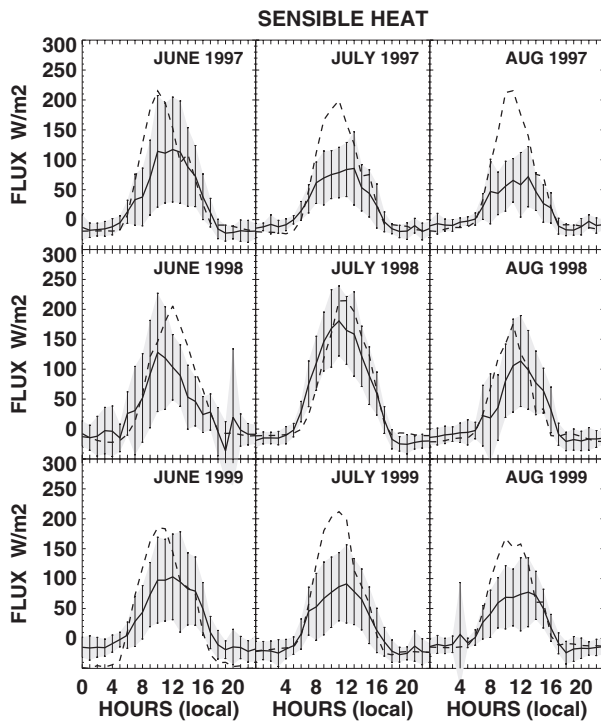


Fig. 2 Diurnal composites of model and observed sensible heat fluxes for summer months during the years 1997–1999. In all panels model data is the dashed line, observed the solid line. Shaded area indicates  $\pm 1$  standard deviation of the mean of the observations.

A composite of the 9 months of summer  $H$  (not shown) revealed that between 08:00 and 12:00 hours, the LST model  $H$  was generally 85–100% larger than observed values. In the afternoon, model  $H$  compared more favorably to observed  $H$ , but was still larger in magnitude by around 40%. The best comparison between modeled and observed  $H$  was in 1998, when the forest was dry. Observed sensible heat flux peaks in July were almost double the values seen during 1997 or 1999, and August 1998  $H$  flux was high as well. In other years the simulated daily peak values exceed observed values, sometimes by a factor of 2 or more.

Hourly composites of summertime daylight Bowen ratio are shown in Fig. 3. In 1997 and 1999, SiB values are approximately twice observed, while in 1998 simulated and observed Bowen ratios are similar. Some explanations for the Bowen ratio discrepancy, when taken with the data from Figs 1 and 2, are (a) systematic overestimation of net radiation in SiB, possibly resulting from underestimation of the broadband solar albedo; (b) underestimation of heat flux into the soil by SiB; (c) underestimation of observed sensible heat fluxes by the eddy covariance system; or (d) some combination of these explanations.

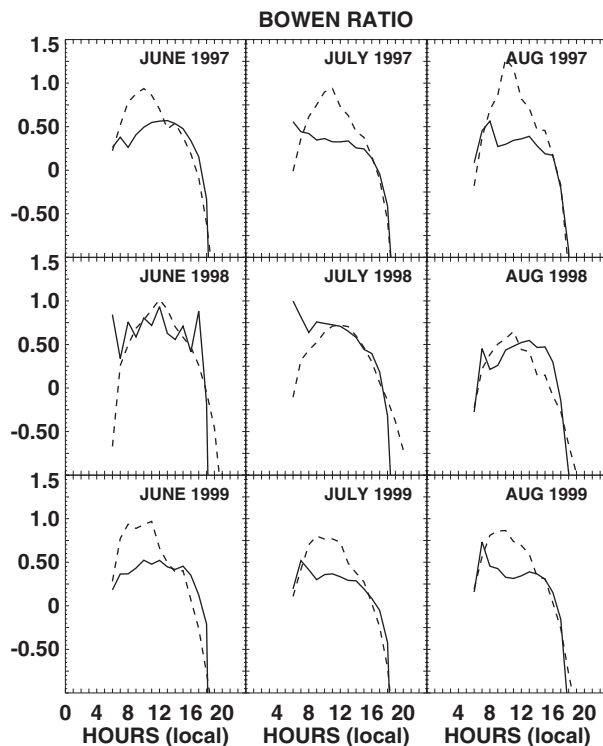


Fig. 3 Diurnal composites of model and observed Bowen ratio, daylight hours, for summer months during the years 1997–1999. In all panels model data is dashed line, observed the solid line.

Several authors (Desjardins *et al.*, 1997; Mahrt, 1998; Twine *et al.*, 2000; Davis *et al.*, this issue) have noted that observed latent and sensible fluxes are generally undermeasured by 10–30% by eddy covariance instruments at flux towers, and that observed energy budgets often fail to achieve closure. However, across-the-board increases of  $H$  and LE will not result in a more favorable comparison between model and observations, which is easily seen in Figs 1 and 2. That the observed and simulated Bowen ratios often differ by a factor of 2 (Fig. 3) suggests that there are fundamental differences between the energy partition in the model and that observed at the tall tower.

By design, the energy budget within the model is perfectly balanced ( $R_n - H - LE - G = 0$ ). Simulated LE was generally in good agreement with the observations, yet simulated  $H$  was often much greater than that observed. This implies that either  $R_n$  was overestimated in the model, or  $G$  was underestimated, or both. Net radiation measurements made at the base of the tall tower do not represent the forested ecosystem that defines the flux footprint, since they are made less than 2 m above the mowed grass clearing in which the TV tower is anchored. Radiative forcing was applied to SiB using measurements of down-

ward solar and estimated longwave radiation at the tower. Solar radiation was parsed into visible and near-IR components, and radiative transfer within the model was computed using a two-stream approximation (Sellers, 1985). For several months in 1998, data from a four-component radiometer were available for a forested site close to the WLEF tower (Willow Creek).

The model underestimates reflected July solar radiation by about  $60 \text{ W m}^{-2}$  at mid-day in the monthly mean (not shown). This error was due to under-

estimation of albedo (9.3% at mid-day in SiB vs. 16.5% at Willow Creek), which is not too surprising given the heterogeneous vegetation cover in the area—the mowed grass where the observations were taken would have considerably less albedo than the forest. Downward longwave radiation exhibits more diurnal variation in the observations than in the prescribed meteorological driver data (derived from air temperature and humidity), and upward longwave in the model was greater than the observations during the day. These errors largely cancel the error in reflected

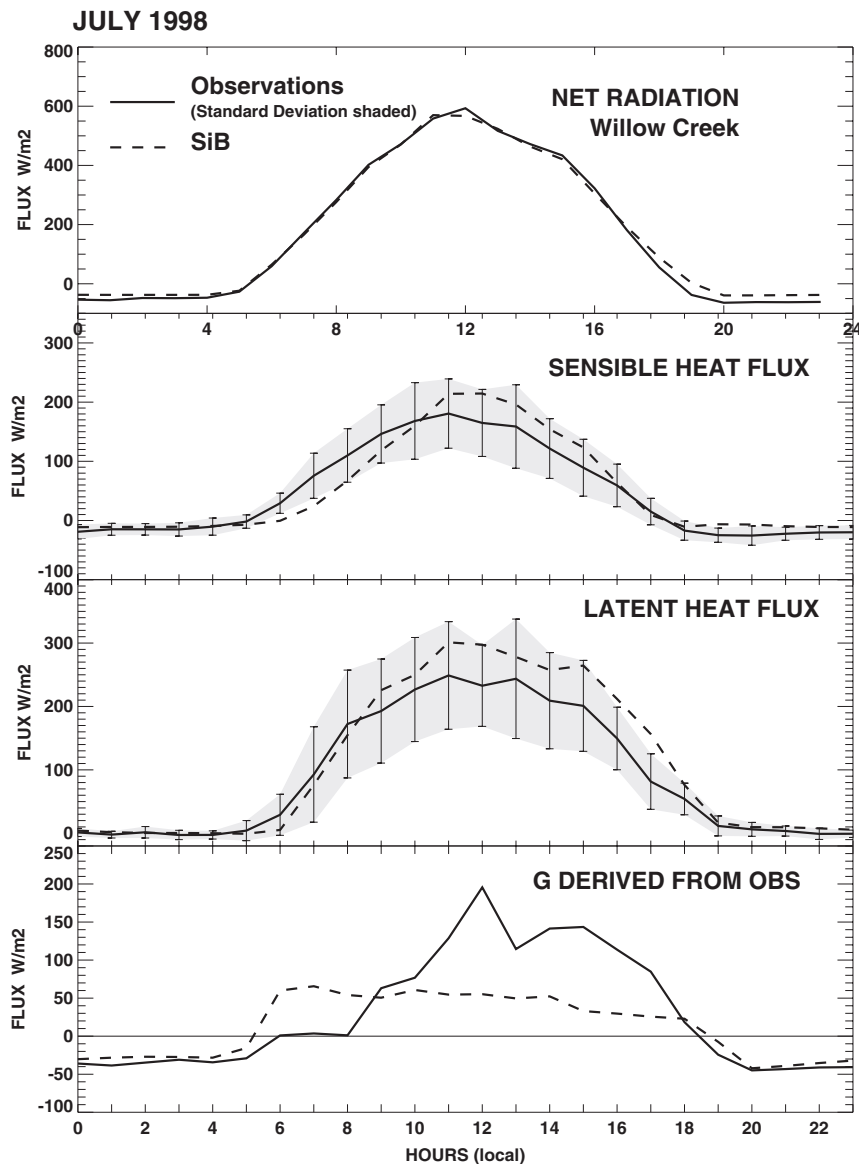


**Fig. 4** Diurnal composite of comparison of model and observed net radiation, sensible heat flux, latent heat flux and model ground heat flux vs. 'residual' ground heat flux from observations for July, 1998. In all panels model data is dashed line, observed data the solid line. In panels 2 and 3 the shaded area indicates  $\pm 1$  standard deviation of the mean of the observations.

solar radiation, with the result that the model captures the average diurnal variations in the net radiation components very well (top panel, Fig. 4).

The energy balance can be evaluated using the four-component radiometer, the latent and sensible heat flux data (all from Fig. 4), and the energy closure assumption

$$G_{\text{residual}} = R_n - H - LE$$

to calculate a residual ground heat flux for the observations. The net radiation ( $R_n$ ) and latent, sensible, and ground fluxes are shown in Fig. 4. The ground heat flux is explicitly calculated in SiB, while the energy

budget closure is assumed to obtain the observed  $G_{\text{residual}}$ . In July 1998, the diurnal composite of model  $G$  peaks at around  $60 \text{ W m}^{-2}$  shortly after sunrise, then slowly drops to near zero by sunset. The observed  $G_{\text{residual}}$  remains at zero until 2 h after sunrise, then rises to near  $200 \text{ W m}^{-2}$  at mid-day, which is quite high, even with the assumed underestimation of  $H$  and  $LE$  factored in.

Simulated values of  $G$  may also be too weak. Observations of soil temperature were taken at the surface as well as 5, 10, 20, and 50-cm depths. Figure 5 shows the temperature profiles for the observational and SiB data, as well as the difference between the

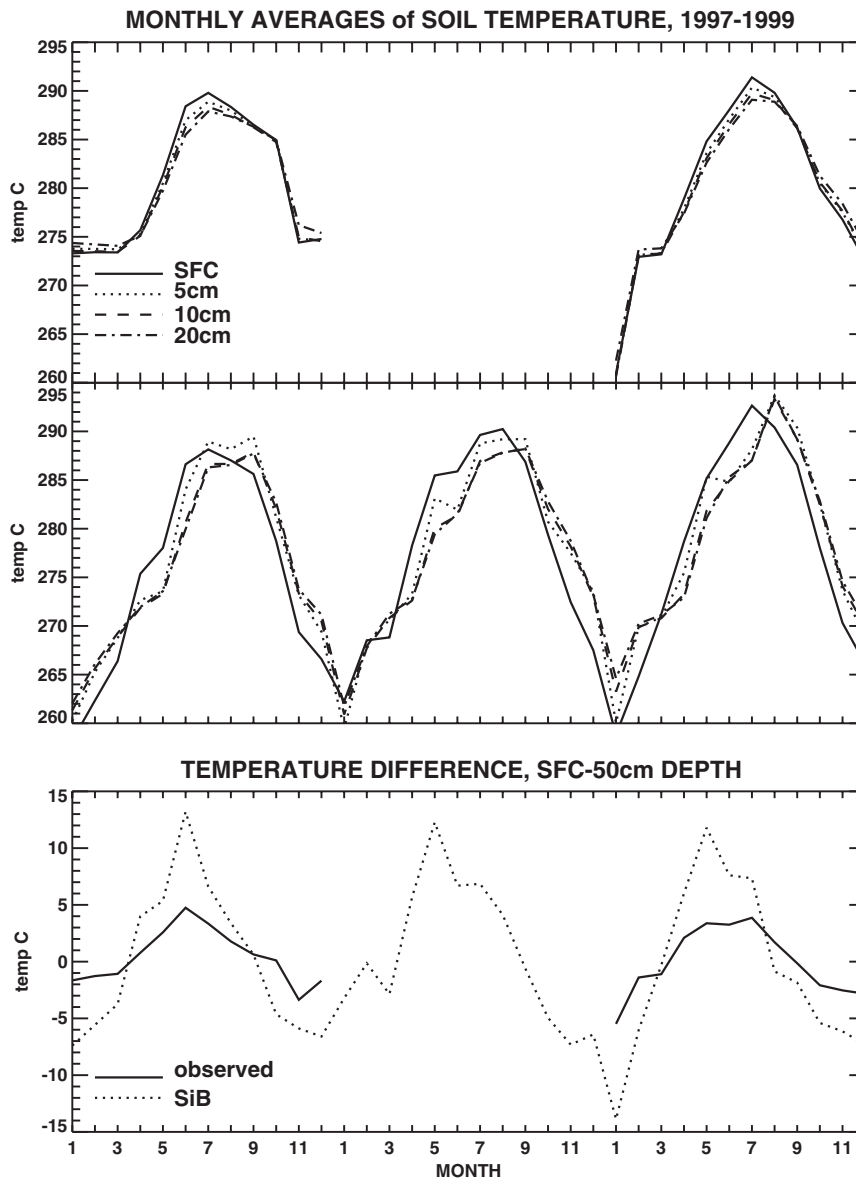
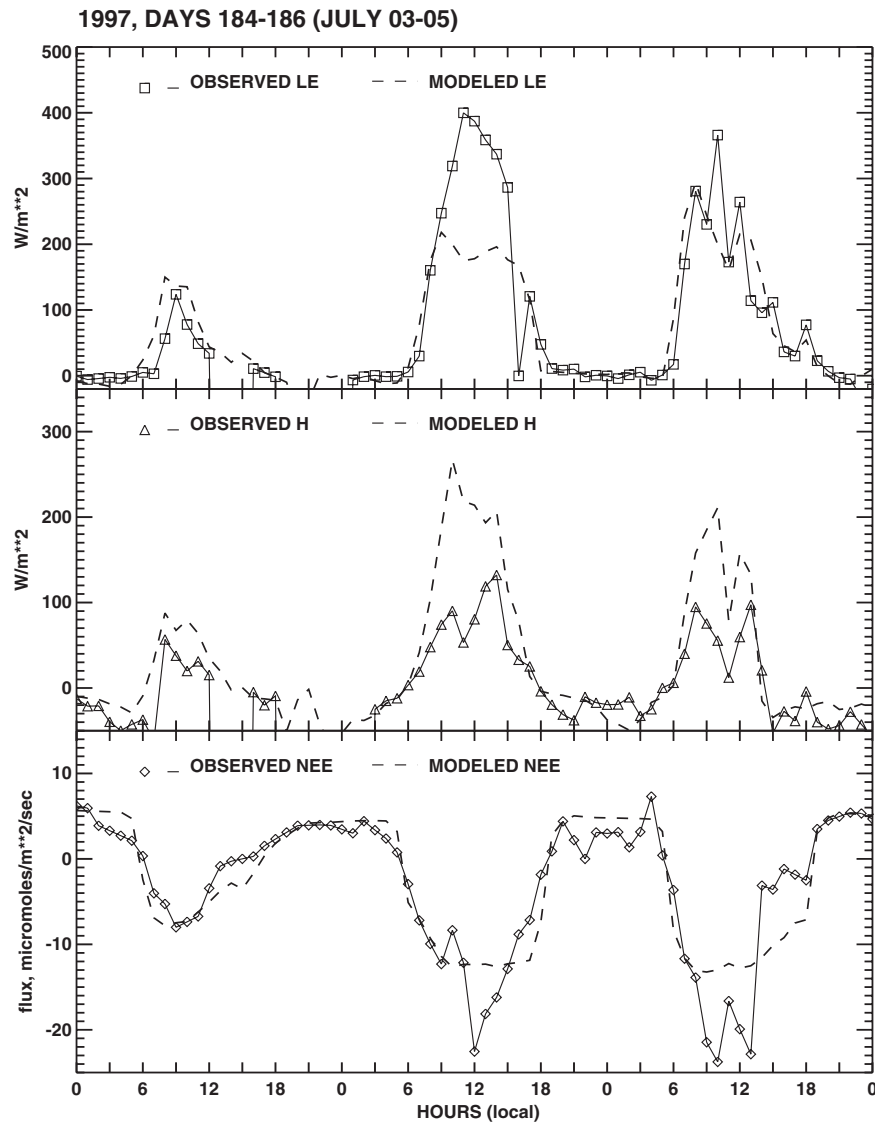


Fig. 5 Monthly averages of soil temperature at surface and layers 5, 10, 20 and 50 cm deep (top panel observed, second panel SiB), as well as temperature difference between surface and 50 cm depth (bottom panel).

surface and 50-cm depth. SiB soil temperature data were interpolated to match observation depths. A notable difference between the simulated soil temperature and observations is the timing of extrema: monthly mean observed soil temperatures attain their highest (and lowest) yearly values in the same month for all levels. The SiB data revealed an offset of 1–2 months between extreme values at the surface and at depth. Also, the strength of the temperature gradient in the observed soil is much smaller than simulated. A 10–15°C difference between the surface and 50 cm is common in the model in both summer and winter, while the observed gradient rarely exceeds 5°. The

strong thermal gradient in the model suggests that heat flux within the soil is unrealistically weak.

When likely underestimation of observed fluxes is taken into account, then the SiB-tower comparison can be summarized as follows: model LE is close to or even slightly smaller than observed, model  $H$  is much larger than observed, and  $G_{\text{residual}}$  calculated from observations is much larger than simulated. A potential explanation from these differences may lie in the wetlands in the region of the WLEF tower. In a comparison of aircraft with tower data at BOREAS (Desjardins *et al.*, 1997), it was noted that the aircraft fluxes were generally smaller than those observed at a



**Fig. 6** Time series of 3 days of modeled and observed fluxes in July 1997. Top panel is latent heat, middle panel sensible heat, bottom panel net ecosystem exchange. In all panels dashed line is model data, solid line observed.

tower due to the fact that the tower was located in a dry area, while the aircraft flew over both dry and wetland areas. The tower in the BOREAS study was only 20 m tall, and the suggestion was that the tower footprint encompassed mostly dry upland areas, while the aircraft flew over wetlands more representative of the region. In the BOREAS study, the wetlands LE sampled by the aircraft was similar to or larger than the LE observed at the 'dry' tower, while wetlands *H* was much smaller. At WLEF, the tower is tall enough (fluxes sampled at 30, 122, and 396 m) such that the footprint is of the order of 24 km<sup>2</sup>, and therefore contains some of the considerable wetlands that surround the tower. In SiB, however, wetlands are not simulated. Model phenology is determined by vegetation maps, which do not currently contain wetlands as a vegetation type.

Figure 6 shows a time series of 3 days in July 1997 (Julian days 184–186). On the first day (184) conditions were cool and rainy. Model and observed *H* and LE compare quite closely with each other, likely because all surfaces were wet and differences between the observed canopy/wetlands and model canopy would be minimized. Rainfall ended on the morning of day 185, and while large latent heat fluxes were observed, the

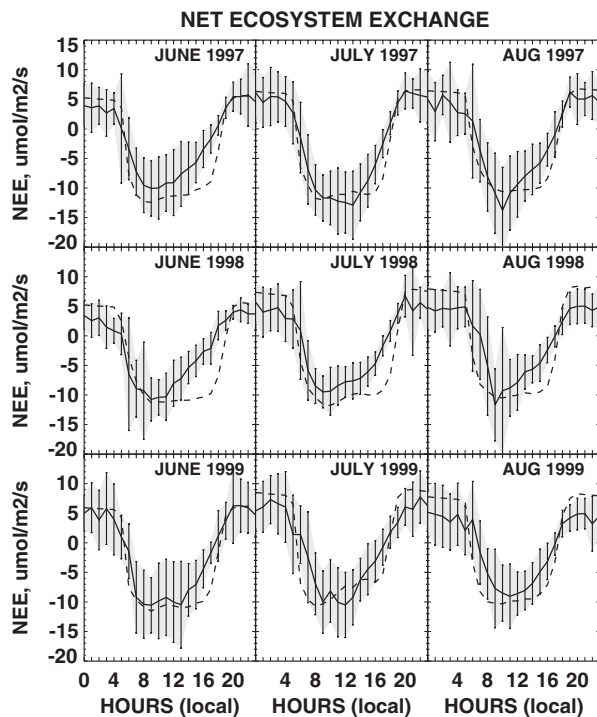


Fig. 7 Diurnal composites of model and observed net ecosystem exchange of carbon for summer months during the years 1997–1999. In all plots model data is the dashed line, observed the solid line. Shaded area indicates  $\pm 1$  standard deviation of the available observations.

model partitioned more of its energy into sensible heat. This is likely due to the fact that runoff that would form pools and puddles in the observed forest is removed immediately from the model once it exceeds storage capacity limits. As the area dries out by day 186, the flux comparison more closely resembles monthly mean values, where model LE is similar to that observed and model *H* is much larger.

The mean diurnal cycles of simulated CO<sub>2</sub> flux compared favorably with observations during the summer months (Fig. 7). In general, SiB captured the behavior of the initial drawdown of carbon following sunrise, although there was a slight tendency to overestimate morning carbon flux into the canopy. Daily peak assimilation rates were simulated quite well. In many months, SiB exhibited excessive respiration at night (June 1997 being the exception), and had a tendency to maintain vigorous photosynthesis well into late afternoon, at times when the observed canopy carbon flux was near zero or even positive.

During the growing season, the model consistently simulated excessive photosynthesis and transpiration in the late afternoon, after the observations showed decreased canopy activity. Canopy radiative transfer for the calculation of heating rates in SiB is treated using a two-stream approximation that includes separate contributions of direct and diffuse radiation in visible and near-infrared wavelengths (Sellers *et al.*, 1985). Photosynthesis calculations and scaling from leaf to canopy, however, are performed using monthly mean extinction coefficients derived from projected leaf areas. This facilitates the use of monthly composited NDVI data to derive scaling parameters (Sellers *et al.*, 1992, 1996a), but means that within-canopy extinction of PAR does not vary diurnally. Also, the effects of shading and diffuse radiation are not explicitly treated in the current model. A revised canopy radiation model that includes diurnally varying geometry for canopy radiation would likely result in somewhat enhanced photosynthesis and latent heat fluxes at mid-day, and a gradual reduction of canopy activity in late afternoon and evening as light levels fall.

Model performance during spring months was highly variable, and the degree of agreement with observations varied as well. Simulations for the spring months showed a tendency to overestimate springtime assimilation, both in the magnitude of diurnal cycles and in the 'bud-burst' or activation of the canopy. In May 1998, the simulations matched the observations well; in May 1997 and 1999 the model signal was overestimated. In all 3 years the April assimilation signal was quite obvious in the simulations, while only very weak in the observations, and weak daytime assimilation was even simulated in March 1998 and 1999.

For the present study, all 3 years simulated used vegetation parameters based upon 1995 1-km AVHRR data. Our preference would be to use satellite data from the appropriate years, but unfortunately these data were not available for 1997–1999. Specifying canopy phenology from NDVI data is intended to allow the model to capture spatial and interannual variations, but the simulated canopy was obviously much more active in early spring than was the case in the observations. The AVHRR data used for canopy phenology for all 3 years of the simulation was 1995, during which leaf-out was relatively late. Some of this discrepancy may be the result of the very different spatial scale of the NDVI; at the 1-km scale of the NDVI data, the site is quite heterogeneous and includes

evergreen trees that would account for a higher LAI in early spring. To minimize artifacts from cloud contamination and other atmospheric interference, the NDVI data were treated as monthly maximum-value composites assigned to the middle of each month. Thus May NDVI is likely to reflect conditions at the end of the month, and the procedure for linear interpolation to daily values begins introducing the influence of this May value on April 16. Finally, simulated springtime soil temperatures showed a strong cold bias relative to the observations (Fig. 5). Since soil respiration is exponential with soil temperature, this deficiency nearly eliminated CO<sub>2</sub> efflux from the soil and amplified the error in the simulated springtime NEE.

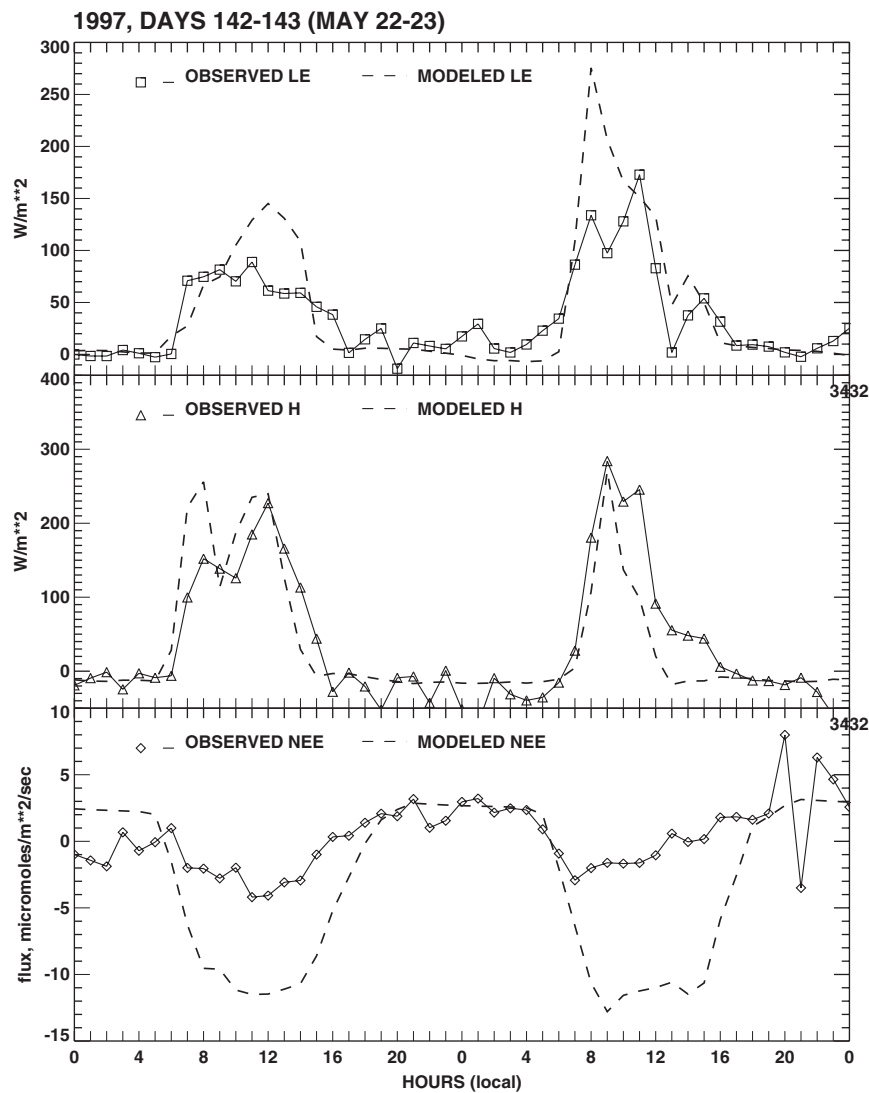


Fig. 8 Time series of latent heat, sensible heat, and carbon flux 22–23 May 1997. Top panel is latent heat, middle panel sensible heat, bottom panel net ecosystem exchange. In all panels dashed line is model data, solid line observed.

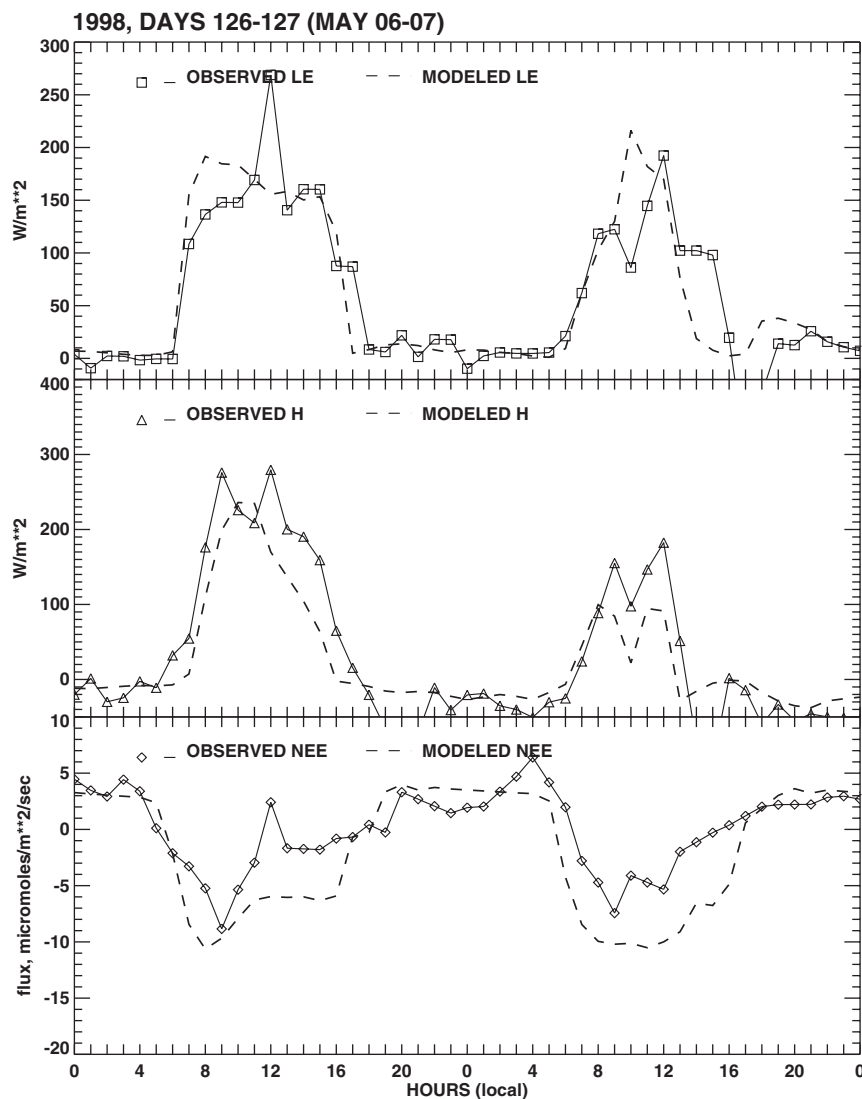
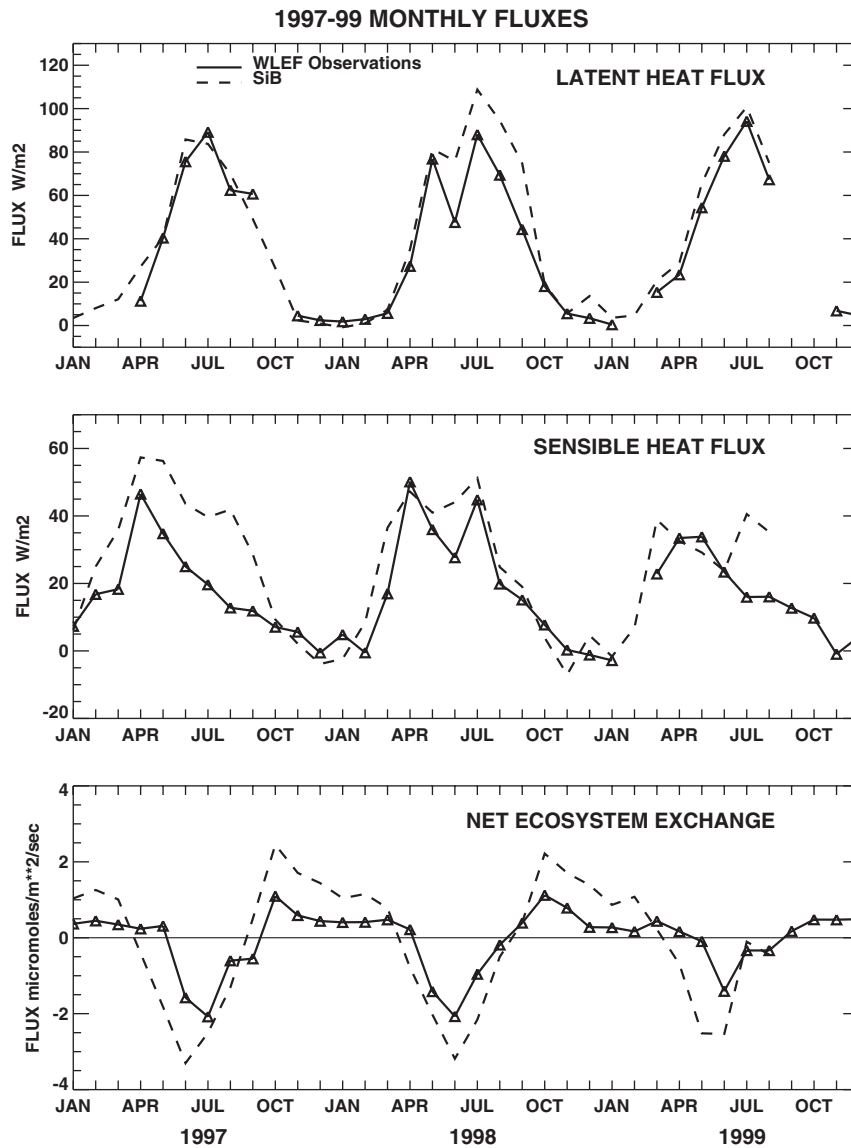


Fig. 9 Time series of latent heat, sensible heat and carbon flux 06–07 May 1998. Top panel is latent heat, middle panel sensible heat, bottom panel net ecosystem exchange. In all panels dashed line is model data, solid line observed.

The dependence of SiB on prescribed phenology is readily apparent in Figs 8 and 9. The bottom panels of Figs 8 and 9 show the NEE for several days in 1997 and 1998. The canopy specification in the model was identical for the 2 years, and maximum assimilation for May in either 1997 or 1998 was around  $-10$  to  $-12 \mu\text{M m}^{-2} \text{s}^{-1}$ . In 1997 (Fig. 8) the observed assimilation peaked around  $-5 \mu\text{M m}^{-2} \text{s}^{-1}$ , and was closer to  $-10$  in 1998 (much closer to modeled values), indicating that there were significant differences in canopy phenology between the two years. The 1998 values of water vapor flux in Fig. 9 show a better comparison to observations than the corresponding fluxes from 1997, highlighting the link between carbon and water vapor fluxes. Measurements of PAR confirm

early leaf-out in 1998, when compared to 1997 and 1999. These LAI differences were probably sufficient to explain the differences in the observed NEE values shown in Figs 8 and 9. However, model-observation comparison was much worse for 22–23 May 1997 than for 6–7 May 1998, which would not be explained wholly by differences in LAI between the model and the actual forest. In late May 1997, the model retained a small amount of snow on the ground, which resulted in decreased soil temperatures when compared to 1998 (not shown). The reduced model soil temperature in 1997 retarded soil respiration. In 1998 all snow was gone from the ground by the 3rd of May, resulting in higher soil temperatures through the column, so soil respiration values increased with the result that peak



**Fig. 10** Monthly mean values of observed and model latent heat flux, sensible heat flux, and net ecosystem exchange of carbon for the years 1997–1999, inclusive. Top panel is latent heat, middle panel sensible heat, bottom panel net ecosystem exchange. In all panels dashed line is model data, solid line observed.

NEE values were less negative, and closer in line with observed values.

#### *Seasonal and interannual variability*

Figure 10 shows monthly averages for latent heat (LE), sensible heat ( $H$ ), and net ecosystem exchange of CO<sub>2</sub> (NEE). Missing data was an issue: some months (January–March 1997) had no observations of LE present, while other months (October 1997, February 1999) had so little  $H$  and/or LE data available that the value of comparison was insignificant. NEE was a more complete record, and as no individual month

contained less than 25% of possible records, all months are shown. It was assumed that the missing observations were randomly spaced throughout the month, and that the monthly mean was not biased by the missing periods. Data filling of the meteorological driver data had only been performed through mid-August 1999, so the model output fluxes for the last quarter of 1999 were not plotted, as they represent fluxes from an averaged or composite climatology as outlined in the data-filling procedures.

The model closely simulated the monthly average of observed latent heat, except in summer 1998. The SiB

simulation captured the annual cycle, as well as interannual variation, with respect to timing/season of maximum and minimum values. Model LE showed greatest deviation from observations during 1998.

The observed annual cycle of sensible heat flux peaked in spring and decreased rapidly until early summer. This decrease coincides with leaf-out, and represents a shift in the Bowen ratio toward increasing transpiration associated with increasing leaf area. Sensible heat flux stabilized from early summer until fall, when the flux dropped to near zero or slightly negative values by mid-winter. Although the simulated  $H$  peaks coincided with observations in the spring (April and May model  $H$  15% and 30% larger than observed), the late spring/summer drop in sensible heat flux was much smaller than observed, with the result that in August 1997 modeled  $H$  was 2.5 times larger than observed values. The simulation produced a secondary peak in July or August that was not seen in the observations save for July 1998. By late summer to early fall, the model  $H$  flux came back into line with observations, and fall and winter simulations were closely matched with the observations.

The magnitude of the simulated NEE was too high in both summer and winter. Observed NEE may have been underestimated during times when the atmosphere was stable (night, winter) due to possible advective carbon losses. The model also mis-timed the springtime shift from net carbon efflux to net uptake, although the timing of the October peak in respiration was correctly simulated.

When available observations were summed over the entire 36-month period, the observed Bowen ratio was 0.53, while the modeled Bowen ratio was much higher, 0.65. This is consistent with the hypothesis of wetlands within the observed flux footprint. The differences between observation-simulation are smallest in the winter when almost all fluxes are from snow-covered surfaces, largest in the spring and summer months.

The model was reasonably successful in capturing variations of fluxes on diurnal, synoptic, and seasonal time scales, but failed to simulate properly differences in the seasonal variations from one year to another. This is likely the result of the use of a single year (1995) of NDVI data to derive phenological variations in physiological parameters such as LAI. The meteorological driver data record, however, was reasonably complete, so we expect to be able to simulate responses to climate anomalies that are present in the data used to force the model.

Vegetation in north-central Wisconsin was in full leaf quite early in the spring in 1998, and by midsummer the canopy was noticeably dry and brown. Precipitation was at near-normal levels in the early part of the year,

but little or no rain fell in June and July, providing a probable reason for canopy desiccation. However, the observed record of these 'drought' conditions of 1998 is not reflected in the flux and NEE observations. NEE of carbon peaked earlier in 1998 than 1997 (June vs. July), but 1999 exhibited a June peak in NEE as well. The monthly mean NEE values (Fig. 10) do not show a significant difference in the magnitude of assimilation between the years, but the monthly diurnal composite data indicated that in 1998 canopy assimilation started slightly later and tended to shut down earlier than in either 1997 or 1999.

The interannual variability in the measured surface fluxes was not well captured by the model, especially in the spring. Changes in canopy phenology, in particular, could not be replicated because of the unavailability of NDVI data for the actual years of the study. This can certainly be remedied as the newer data become available. The most salient feature of the observed interannual variations was the early leaf-out in 1998, which was associated with above-average temperatures during the early spring of that year. The use of monthly maximum NDVI would likely obscure vegetation transformations taking place on temporal scales of days to weeks, with the result that unless time of leaf-out changed by several weeks from one year to the next, the changes may be unnoticed by the model. By late spring/early summer, when the canopy had come into full leaf, the year-to-year differences were due more to atmospheric conditions (atmospheric driver data) than to the phenology prescribed to the model. The senescence of the Wisconsin forest displayed less interannual variation for the 3 years simulated, as comparison of fluxes in the fall of the year did not show the variation seen in the spring. Although the model canopy parameters were identical for 1998 to those of the other 2 years, simulated soil temperatures were higher earlier and simulated soil moisture (not shown) was lower in May and June of 1998 than in 1997 or 1999. These changes were also present in the observations, although in neither the data nor the simulation were these anomalies sufficiently strong to induce much physiological stress: carbon uptake and transpiration were nearly as strong in 1998 as in the other years, although the growing season began earlier.

## Conclusions

The offline simulations of 3 years (1997–1999) of surface fluxes at the WLEF-TV tower by SiB provided an opportunity to assess model performance closely. The intention here was not to produce the most accurate simulation possible: model parameters were not 'tuned' to obtain a better match to observations. Rather, the

simulation was treated as an opportunity to test model performance for a location in which meteorology and fluxes are well observed, but which is otherwise like any other model grid cell. Parameters were estimated from 1-km NDVI data, as has been conducted for a large domain surrounding the tower site. A fully coupled simulation (Denning *et al.*, this issue) uses exactly the same approach, except that the weather is interactive with the simulated biophysics and biogeochemistry, being simulated in a mesoscale model.

Overall, the model was reasonably successful in capturing variations in fluxes of latent and sensible heat and CO<sub>2</sub> at the WLEF-TV site over diurnal, synoptic, and seasonal time scales. The agreement between the model and the observations was particularly good for latent heat flux, but less good for sensible heat flux and net carbon exchange. Simulated sensible heat flux was generally greater than observed. Analysis of surface energy budget components suggests that this disagreement may reflect a combination of errors in model albedo and soil thermal conductivity, and underestimation by the eddy flux system. Furthermore, the presence of wetlands within the flux footprint, and absence of wetlands in the SiB simulation provide a possible explanation for some of the differences in the model-observations comparison. As described by Desjardins *et al.* (1997) wetlands would result in larger ground heat flux and smaller sensible heat flux; if these mechanisms were included in the simulation, the Bowen ratio would shift towards values closer to those observed.

As a test, a simple wetlands configuration was coded into SiB by forcing all soil levels to saturation and prescribing a thin layer of water at the surface. Vegetation was set as grass, and the code was run using the WLEF driver data. The goal was to provide a parameterization that would partition latent and sensible heat at a lower Bowen ratio, one more representative of wetlands. The summer mid-day mean Bowen ratio for years 1997–1999 was 0.60 for the initial SiB runs, 0.15 for the modified SiB ‘wetland’ runs, and 0.43 for the observations. When the wetland-modified SiB runs were tiled in with the standard runs, the modeled and observed Bowen ratio are equal at slightly more than 35% wetland, which compares favorably with the observed amount of wetlands (40%) cited by Mackay *et al.* (this issue).

The modified SiB wetland was not meant to be a solution to the SiB Bowen ratio discrepancy with the observations, but merely a tool to support the hypothesis that wetlands affect the fluxes within the tower footprint. Wetlands in the region of the WLEF tower are not static in nature, as can be seen in Fig. 3. In a dry year (1998, middle row), the observed Bowen ratio was very close to the SiB Bowen ratio with no modeled

wetland influence, while in other years (1997, 1999) the modeled Bowen ratio (no wetland influence) was almost twice that observed. Obviously, if wetlands are to be correctly simulated in SiB, variables such as vegetation type and fraction, water level, and water temperature must be taken into account. Interannual variability was less well simulated, especially in springtime, due to the unavailability of NDVI data for parameterization of canopy properties during the actual years of the study. Interannual variability during summertime, when the canopy was in full leaf, was more successfully simulated given changes in climatic drivers.

The model consistently overestimated late-day photosynthesis and transpiration relative to the observations, typically producing ‘U-shaped’ diurnal cycles, whereas the observed diurnal cycle was more typically ‘V-shaped’. This was likely due to the model’s treatment of within-canopy light extinction, which was appropriate for diffuse light but failed to represent shading and extinction of direct-beam radiation correctly. The radiative transfer submodel essentially treats all light within the canopy as diffuse, resulting in an unrealistically high canopy-average light-use efficiency.

The highest priority for model improvement is placed on canopy radiative transfer, soil thermodynamics, and obtaining better NDVI data sets for this period. In a companion paper (Denning *et al.*, this issue), we proceed to test the current model in a fully coupled mode in a set of mesoscale simulations.

### Acknowledgements

This research was funded by the South-Central Regional Center (SCRC) of the National Institute for Global Environmental Change (NIGEC) through the US Department of Energy (Tul-066-98/99 Modification #1 and Tul-106-00/01) and through the US Department of Energy Contract DE-FG03-02ER63474 A001. Support was also received through a subcontract from the University of California at Berkeley (SA 2805-23941, Amd. 4). The Atmospheric Chemistry Project of the Climate and Global Change Program of NOAA supported observations taken at the WLEF-TV tower. Thanks are also due to Ron Teclaw of the USDA Forest Service Forestry Science Laboratory in Rhinelander, WI for assistance in maintaining the WLEF site, and to Roger Strand, chief engineer of WLEF-TV and the State of Wisconsin Educational Communications Board for allowing us to use the tall tower. Any opinions, findings, and conclusions or recommendations expressed herein are those of the authors and do not necessarily reflect the view of the DOE.

### References

- Atlas RM, Wolfson N (1993) The effect of SST and soil moisture anomalies on GLA model simulations of the 1988 U.S. summer drought. *Journal of Climate*, **6**, 2034–2048.

- Bakwin PS, Tans PP, Hurst DF *et al.* (1998) Measurements of carbon dioxide on very tall towers: results of the NOAA/CMDL program. *Tellus*, **50B**, 401–415.
- Beljaars ACM, Viterbo PA, Miller MJ *et al.* (1996) The anomalous rainfall over the United States during July 1993: sensitivity to land surface parameterization and soil moisture anomalies. *Monthly Weather Review*, **124**, 362–383.
- Berger BW, Davis KJ, Yi C *et al.* (2001) Long-term carbon dioxide fluxes from a very tall tower in a northern forest: flux measurement methodology. *Journal of Atmospheric and Oceanic Technology*, **18**, 529–542.
- Betts AK, Ball JH, Beljaars ACM *et al.* (1996) The land surface-atmosphere interaction: a review based on observational and global modeling perspectives. *Journal of Geophysical Research*, **101**, 7209–7225.
- Betts AK, Viterbo PA, Beljaars ACM *et al.* (1998) Evaluation of land-surface interaction in ECMWF and NCEP/NCAR reanalysis models over grassland (FIFE) and boreal forest (BOREAS). *Journal of Geophysical Research*, **103**, 23079–23085.
- Bonan GB (1996) *A land surface model (LSM Version 1.0) for ecological, hydrological, and atmospheric studies: technical description and user's guide*. NCAR Technical Note NCAR/TN-417 + STR.
- Bonan GB (1998) The land surface climatology of the NCAR land surface model coupled to the NCAR community climate model. *Journal of Climate*, **11**, 1307–1326.
- Bousquet P, Ciais P, Peylin P *et al.* (1999a) Inverse modeling of annual atmospheric CO<sub>2</sub> sources and sinks, part 1: method and control inversion. *Journal of Geophysical Research*, **104**(D21), 26161–26178.
- Bousquet P, Peylin P, Ciais P *et al.* (1999b) Inverse modeling of annual atmospheric CO<sub>2</sub> sources and sinks, Part 2: sensitivity study. *Journal of Geophysical Research*, **104**(D21), 26179–26193.
- Clapp RB, Hornberger GM (1978) Empirical equations for some soil hydraulic properties. *Water Resources Research*, **14**, 601–604.
- Collatz GJ, Ball JT, Grivet C *et al.* (1991) Physiological and environmental regulation of stomatal conductance, photosynthesis, and transpiration: a model that includes a laminar boundary layer. *Agricultural and Forest Meteorology*, **54**, 107–136.
- Collatz GJ, Ribas-Carbo M, Berry JA (1992) Coupled photosynthesis-stomatal conductance model for leaves of C<sub>4</sub> plants. *Australian Journal of Plant Physiology*, **19**, 519–538.
- Colello GD, Grivet C, Sellers PJ *et al.* (1998) Modeling of energy, water, and CO<sub>2</sub> flux in a temperate grassland ecosystem with SiB2: May–October 1987. *Journal of the Atmospheric Sciences*, **55**, 1141–1169.
- Davis KJ, Bakwin PS, Yi C *et al.* (2003) The annual cycles of CO<sub>2</sub> and H<sub>2</sub>O exchange over a northern mixed forest as observed from a very tall tower. *Global Change Biology*, **9**, 1278–1293.
- Denning AS, Fung IY, Randall DA (1995) Latitudinal gradient of atmospheric CO<sub>2</sub> due to seasonal exchange with land biota. *Nature*, **376**, 240–243.
- Denning AS, Collatz JG, Zhang C *et al.* (1996a) Simulations of terrestrial carbon metabolism and atmospheric CO<sub>2</sub> in a general circulation model. Part 1: surface carbon fluxes. *Tellus*, **48B**, 521–542.
- Denning AS, Randall DA, Collatz GJ *et al.* (1996b) Simulations of terrestrial carbon metabolism and atmospheric CO<sub>2</sub> in a general circulation model. Part 2: spatial and temporal variations of atmospheric CO<sub>2</sub>. *Tellus*, **48B**, 543–567.
- Denning AS, Takahashi T, Friedlingstein P (1999) Can a strong atmospheric CO<sub>2</sub> rectifier effect be reconciled with a 'reasonable' carbon budget? *Tellus*, **51B**, 249–253.
- Denning AS, Nicholls M, Prihodko L *et al.* (2003) Simulated and observed variations in atmospheric CO<sub>2</sub> over a Wisconsin forest using a coupled Ecosystem-Atmosphere Model. *Global Change Biology*, **9**, 1262–1277.
- Desjardins RL, MacPherson JI, Mahrt L *et al.* (1997) Scaling up flux measurements for the boreal forest using aircraft-tower combinations. *Journal of Geophysical Research*, **102**, 29125–29133.
- Fan S, Gloor M, Mahlman J *et al.* (1998) A large terrestrial carbon sink in North America implied by atmospheric and oceanic carbon dioxide data and models. *Science*, **282**, 442–446.
- Farquhar GD, von Caemmerer S, Berry JA (1980) A biochemical model of photosynthetic CO<sub>2</sub> assimilation in C<sub>3</sub> plants. *Planta*, **14**, 78–90.
- Gurney KR, Law RM, Denning AS *et al.* (2002) Towards robust regional estimates of CO<sub>2</sub> sources and sinks using atmospheric transport models. *Nature*, **415**, 626–662.
- Hansen MC, DeFries RS, Townshend JRG *et al.* (2000) Global land cover classification at 1 km spatial resolution using a classification tree approach. *International Journal of Remote Sensing*, **21**, 1331–1364.
- Idso SB (1981) A set of equations for full spectrum and 8 mm to 14 mm and 10.5 mm to 12.5 mm thermal radiation from cloudless skies. *Water Resources Research*, **17**, 295–304.
- Los SO, Collatz GJ, Sellers PJ *et al.* (2000) A global 9-yr biophysical land surface dataset from NOAA AVHRR data. *Journal of Hydrometeorology*, **1**, 183–199.
- Mackay DS, Ahl DE, Ewers BE *et al.* (2003) Effects of aggregated classifications of forest composition on estimates of evapotranspiration in a northern Wisconsin forest. *Global Change Biology*, (in press).
- Mahrt L (1998) Flux sampling errors for aircraft and towers. *Journal of Atmospheric and Oceanic Technology*, **15**, 416–429.
- Rayner PJ, Enting IG, Francey RJ *et al.* (1999) Reconstructing the recent carbon cycle from atmospheric CO<sub>2</sub>, δ<sup>13</sup>C, and O<sub>2</sub>/N<sub>2</sub> observations. *Tellus*, **B51**, 213–232.
- Sellers PJ (1985) Canopy reflectance, photosynthesis, and transpiration. *International Journal of Remote Sensing*, **6**(8), 1335–1372.
- Sellers PJ, Mintz Y, Sud YC *et al.* (1986) A simple biosphere model (SiB) for use within general circulation models. *Journal of the Atmospheric Sciences*, **43**, 505–531.
- Sellers PJ, Dorman JL (1987) Testing the simple biospheric model (SiB) using point micrometeorological and biophysical data. *Journal of Climate and Applied Meteorology*, **26**, 622–650.
- Sellers PJ, Shuttleworth WJ, Dorman JL *et al.* (1989) Calibrating the simple biosphere model for Amazonian tropical forest using field and remote sensing data. Part I: average calibration with field data. *Journal of Applied Meteorology*, **28**, 727–759.
- Sellers PJ, Heiser MD, Hall FG (1992) Relations between surface conductance and spectral vegetation indices at intermediate (100 m<sup>2</sup> to 15 km<sup>2</sup>) length scales. *Journal of Geophysical Research*, FIFE Special Issue, **97**, 19033–19059.

- Sellers PJ, Randall DA, Collatz GJ *et al.* (1996a) A revised land surface parameterization (SiB2) for atmospheric GCMs. Part I: model formulation. *Journal of Climate*, **9**, 676–705.
- Sellers PJ, Los SO, Tucker CJ *et al.* (1996b) A revised land surface parameterization (SiB2) for atmospheric GCMs. Part II: the generation of global fields of terrestrial biophysical parameters from satellite data. *Journal of Climate*, **9**, 706–737.
- Sellers PJ, Meeson BW, Closs J *et al.* (1996c) The ISLSCP initiative I global datasets: surface boundary conditions and atmospheric forcings for land-atmosphere studies. *Bulletin of the American Meteorological Society*, **77**, 1987–2006.
- Sellers PJ, Dickinson RE, Randall DA *et al.* (1997) Modeling the exchanges of energy, water, and carbon between the continents and the atmosphere. *Science*, **275**, 502–509.
- Sen LS, Shuttleworth WJ, Yang ZL (2000) Comparative evaluation of BATS2, BATS, and SiB2 with Amazon data. *Journal of Hydrometeorology*, **1**, 135–153.
- State Soil Geographic Database (STATSGO) (1994) *US Department of Agriculture, Natural Resources Conservation Service*. Fort Worth, Texas.
- Teillet PM, El Saleous N, Hansen MC *et al.* (2000) An evaluation of the global 1-Km AVHRR land dataset. *International Journal of Remote Sensing*, **21**, 1987–2021.
- Twine TE, Kustas WP, Norman JM *et al.* (2000) Correcting eddy-covariance flux underestimates over a grassland. *Agricultural and Forest Meteorology*, **103**, 279–300.
- Uliasz M (2000) A modeling approach to evaluate aircraft sampling strategies for estimation of terrestrial CO<sub>2</sub> fluxes. In: *14th Symposium on Boundary Layer and Turbulence, 7–11 August, 2000, Aspen, CO*, pp. 630–632. American Meteorological Society, Boston.
- Viterbo P, Bejaars ACM (1995) An improved land surface parameterization scheme in the ECMWF model and its validation. *Journal of Climate*, **8**, 2716–2748.
- Zhang C, Dazlich DA, Randall DA *et al.* (1996) Calculations of the global land surface energy, water, and C fluxes with an off-line version of SiB2. *Journal of Geophysical Research*, **101**, 19061–19075.